

# Scalings of the synchrotron cut-off and turbulent correlation of active galactic nucleus jets

Mitsuru Honda<sup>1</sup>

<sup>1</sup>*Plasma Astrophysics Laboratory, Institute for Global Science, Mie, Japan*

Accepted 2010 July 15. Received 2010 June 24; in original form 2010 February 4

## ABSTRACT

We propose a new analytic scaling of the cut-off frequency of synchrotron radiation from active galactic nucleus (AGN) jets that are nonuniformly filled with many filaments. The theoretical upper limit is provided independent of magnetic intensity, spectral index, coherence and correlation length of filamentary turbulence, etc., such that  $\nu_c \simeq 6 \times 10^{20} \delta [(r-1)/r]^{4/3} (b/10^{-4})$  Hz, where  $\delta$ ,  $r$  and  $b$  are the Doppler beaming factor, shock-compression ratio and energy-density ratio of the perturbed/local mean magnetic field of the filaments, respectively. Combining our results with observational data for 18 extragalactic sources, a constraint on the filament correlation length is found, in order to give the number scaling of filaments. The results suggest that, in particular, the jets of compact BL Lacs possess a large number of filaments with transverse size scale smaller than the emission-region size. The novel concept of the quantization of flowing plasma is suggested.

**Key words:** acceleration of particles – radiation mechanisms: non-thermal – turbulence – methods: analytical – galaxies: evolution – galaxies: jets.

## 1 INTRODUCTION

The pronounced extension of the synchrotron radio continuum to the X-ray region, not formerly predicted, is now known to be a very common feature among radio jets (e.g. Harris & Krawczynski 2006). The crucial point that should be emphasized is that, in many sources, still no clear signs of sharp cut-off are found in the *Chandra* regime (e.g. 3C 66B: Hardcastle et al. 2001; M87: Marshall et al. 2002; 3C 31: Hardcastle et al. 2002; M84: Harris et al. 2002; 3C 346: Worrall & Birkinshaw 2005), and there is even an implication of the possible appearance of a gamma-ray tail in the synchrotron spectral component. This fact is of considerable interest, directly related to the challenging issue of how high an energy range electrons could be accelerated up to in situ. In a conventional fashion, the electron energy distribution is truncated at an assumed ‘highest energy’, which could be responsible for the observed spectrum. Independent of such a makeshift solution, however, it is desirous to elaborate on a particle acceleration theory that can naturally account for the extended continuum, with reference to the morphological details innovated by the recent very-long-baseline interferometry survey (e.g. Lobanov & Zensus 2001). From another point of view, theoretical expansion would also be requisite for corroborating a unified scheme of radio-loud active galactic nuclei (AGNs; Urry & Padovani 1995). None the less, the related thorough study required to elucidate a universal mechanism underlying the many

appearances of the energetic continuum has not been performed as yet.

In a simplistic model assuming a homogeneous magnetic field over a particular system, Biermann & Strittmatter (1987) first considered a combination of small pitch-angle scattering diffusion and Fermi-type acceleration of electrons to evaluate the frequency of synchrotron emission from the highest energy electron:

$$\nu_c = 3 \times 10^{14} [3\bar{b}(U/c)^2] \text{ Hz}, \quad (1)$$

where  $U$ ,  $c$  and  $\bar{b}$  ( $< 1$ ) are the shock speed, the speed of light and the ratio of the perturbed to the mean energy density of the global magnetic field, respectively. Although a symptom of cut-off in the range of equation (1) has been suggested in some earlier publications (e.g. Keel 1988; Pérez-Fournon et al. 1988; Meisenheimer et al. 1996), the broad-band spectral fitting is now found to, if anything, entail a break followed by the aforementioned high-energy extension, unlike a sharp cutoff. A clue aiding in achievement of the required higher acceleration efficiency might be the fine structure like filaments inside jets, which can be reconciled with the observational detailed morphology. Based on this notion, Honda & Honda (2005a) have investigated the root-mean-square (rms) diffusion of electrons in inhomogeneous magnetic fields, and found that the intrinsic frequency of the diffuse synchrotron component could reach as high as

$$\nu_c \sim 10^{24} B(\text{mG}) [d(\text{pc})]^{2/3} (U/c)^{4/3} \text{ Hz}, \quad (2)$$

where  $B$  and  $d$  are the rms magnetic field strength and transverse correlation length of filaments, respectively. The relevant argument focusing on the specified case of the nearby M87 jet has been given (Honda & Honda 2007), although the value of  $d$  remained unsolved. Its determination is necessary not only to estimate equation (2) but also complete the filamentary jet model, which could involve various radiation channels (Honda 2008).

This paper has been prepared to spell out explicitly the scalings of the cut-off and break for the dominant synchrotron spectrum established via normal (non-diffuse) processes in filamentary jets, and to revise equation (1), including relativistic beaming effects. Making use of the results, we attempt to extract the scaling of the lower limit of the filament correlation length,  $d_{\text{min}}$ , from observational data for sample extragalactic jets. We find the property that the  $d_{\text{min}}$  value increases as the size of emission regions. A corollary derived from this is that the allowable maximum number (capacity) of filaments with the outer scale ( $\sim d$ ) increases as the propagation distance of the jet increases. For the situation in which AGN jets carry huge currents driven by the central engines of black holes (Appl & Camenzind 1992), we take the current filamentation into consideration in order to calculate the number of filaments ( $N$ ). From comparing  $N$  with the capacity of the outer-scale filaments, we infer the population of fine filaments inside the jets. As a result, it is demonstrated that compact BL Lac objects such as Mrk 421 and 501 would possess typically  $\sim 10^{11}$  filaments with various transverse size scales that are smaller than the entire emission-region size.

## 2 THEORETICAL MODEL AND ANALYSIS

### 2.1 The filamentary jet model

According to the original idea in Honda & Honda (2004), we rely on the hypothesis that a jet consists of many magnetized filaments, accommodated by some radio observations (e.g. Owen et al. 1989). For information, the circumstance concerned is illustrated in Fig. 1. The quasi-stationary magnetic fields are considered to be generated by leptonic currents, and retain an energy-density level comparable to that of the random component of lepton motion (Honda 2007). It is then expected that the Poynting flux level is less than (or, at most, comparable to) the lepton energy flux. In respect of the global energy budget, the small portion that takes part in controlling the transverse dynamics (Section 5) is loaded from the energy reservoir of the jet bulk. If the dominant kinetic energy is carried by hadronic components then an excess of lepton energy departing from the mass ratio (say, 0.05 per cent for a simple electron-proton plasma with no pairs) is entailed in order to generate the currents and magnetic fields, in accord with arguments concerning the power of blazar jets (e.g. Celotti & Ghisellini 2008).

The merging of current filaments can be associated with the inverse cascade of turbulent magnetic energy. For the inertial range of the turbulence, we invoke the phenomenological expression for local magnetic intensity  $|\mathbf{B}| = B_m(\lambda/d)^{(\beta-1)/2}$ , where  $\lambda$  ( $\leq d$ ) is the transverse size of a filament (Fig. 1) and  $\beta$  corresponds to the turbulent spec-

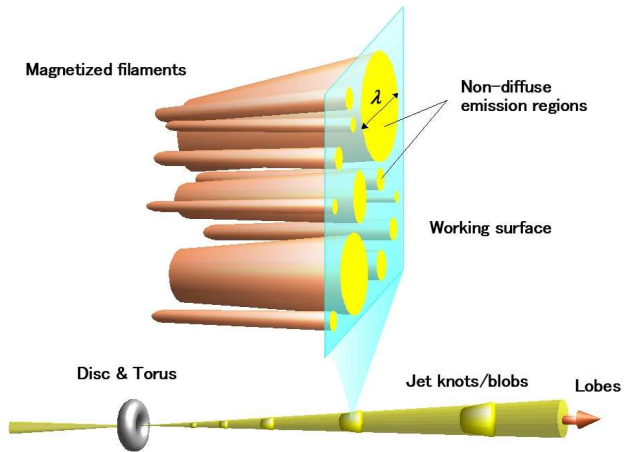


**Figure 1.** Schematic of the AGN jet that contains bright knot-like features associated with shocks. The magnification stands for a local sample around the working surface accompanied by electron acceleration and synchrotron emission.

tral index. As seems plausible, this (zeroth order) magnetic field, trapping lower-energy electrons, is disturbed by Alfvénic waves to allow resonant scattering diffusion. Also, in analogy to the knot and hotspot features, it is reasonable to suppose a relativistic (non-relativistic) shock overtaking the relativistic (non-relativistic) flow with the Lorentz factor  $\Gamma_j = (1 - \beta_j^2)^{-1/2}$ , such that the shock viewed in the upstream rest frame likely has a non-/weakly relativistic speed. Providing the fields defined upstream, we consider the standard diffusive acceleration of bound electrons due to the Fermi-I mechanism (Honda & Honda 2007), which yields a power-law energy distribution ( $\propto \gamma^{-p}$  for  $\gamma \leq \gamma^*$ ).

### 2.2 Updated scalings of break and cut-off frequencies

The acceleration time-scale  $t_{\text{acc}}$  is of the order of the cycle time for one back-and-forth divided by the energy gain per encounter with the shock (e.g. Gaisser 1990). We here adopt a standard expression for  $t_{\text{acc}}$  that involves a negligible contribution from particle escape downstream to the cycle time and gain (Ostrowski 1988; Honda & Honda 2005b). What we deal with below is, therefore, the non-ageing (or flaring) regime around the working surface (a related issue is revisited in Section 3.1). Compatible with this, it is reasonable to suppose that, for major electrons bound to the outer-scale filament with maximum field strength  $\sim B_m$ , the acceleration is degraded by strong synchrotron cooling rather than escape losses (Honda 2008). The synchrotron emission, largely polarized, appears to constitute the dominant radio continuum with a power index of  $\alpha = (p - 1)/2$  in the flux-density spectrum ( $S_\nu \propto \nu^{-\alpha}$ , provided the electron density is uniform, e.g. Longair 1994). The spectral break reflects the highest energy of an accelerated electron ( $\gamma^*|_{\lambda \sim d} mc^2$ ) at which  $t_{\text{acc}}$  is comparable to radiative time-scale. From balancing these time-scales, we can analytically derive the maximum Lorentz factor,  $\gamma_b \equiv \gamma^*|_{\lambda=d}$  (along with the guide-

lines provided in Honda 2008); for convenience, the generic expression is explicitly written as follows:

$$\gamma_b = [f(b, r; B_m, d)]^{1/(3-\beta')} [g(B_m, d)]^{-(1+\beta')/(3-\beta')}. \quad (3)$$

Here,  $b$  is the energy density ratio of the perturbed/local mean magnetic field of filaments, which is assumed to be a constant smaller than unity:  $b \ll 1$  (checked below),  $r$  is the shock-compression ratio,  $\beta' (> 1)$  is the turbulent spectral index of the Alfvénic fluctuations (superimposed on the local mean field) and the dimensionless functions are defined as

$$f \equiv 9\pi^2(\beta' - 1)b \frac{r-1}{r} \frac{B_m d^2}{e}; \quad g \equiv \frac{e B_m d}{2mc^2}, \quad (4)$$

where  $c$ ,  $e$  and  $m$  are the speed of light, elementary charge and electron rest mass, respectively. The observed break frequency can be simply estimated as  $\nu_b = (3/4\pi)\delta\gamma_b^2[eB_m/(mc)]$ , where  $\delta = \Gamma_j^{-1}(1 - \beta_j \cos \theta)^{-1}$  is the beaming factor. When setting the standard value of  $\beta' = \frac{5}{3}$  (for Kolmogorov turbulence), we obtain the scalings

$$\gamma_b = 1.1 \times 10^6 \xi_{-5}^{3/4} B_m^{-5/4} d^{-1/2}, \quad (5)$$

$$\nu_b = 5.2 \times 10^{15} \delta \xi_{-5}^{3/2} B_m^{-3/2} d^{-1} \text{ Hz}, \quad (6)$$

where  $\xi_{-5} = \xi/10^{-5}$  and  $\xi = b[4(r-1)/3r]$ ,  $B_m$  in mG and  $d$  in pc. Note that both equations (5) and (6) are independent of  $\beta$ .

In filaments smaller than  $d$ , the bound electrons can be accelerated up to a higher energy, i.e.  $\gamma^*|_{\lambda < d} > \gamma_b$ , owing to the weaker synchrotron loss. While the synchrotron flux density is lower, the power-law tail is retained up to higher frequency (reflecting the enhanced  $\gamma^*$  value). Apparently, this property can be responsible for the extended continuum going beyond  $\nu_b$ . However, the increase in acceleration efficiency ought to be limited at a critical coherent length  $\lambda_c$ , below which the transverse escape of electrons dominates the radiative loss. In the escape-dominant regime, another  $\gamma^*$  scaling is derived from the spatial limit condition, i.e. equating the electron gyroradius  $r_g$  with  $a(\lambda/2)$ , where  $a$  is a dimensionless factor smaller than unity (see Section 2.3). The equation for  $\gamma^*|_{\lambda < \lambda_c} = \gamma^*|_{\lambda > \lambda_c}$  contains the solution of  $\lambda = \lambda_c$  at which  $\gamma^*$  takes a peak value, to give the expression  $\lambda_c/d = a^{2(3-\beta')/(3\beta+1)} f^{2/(3\beta+1)} g^{-8/(3\beta+1)}$ . Substituting the  $\lambda_c$  expression into the  $\gamma^*$  scaling, the critical Lorentz factor, defined as  $\gamma_c \equiv \gamma^*|_{\lambda=\lambda_c}$ , is obtained as

$$\gamma_c = a^{[(\beta+1)\beta'-2]/(3\beta+1)} f^{(\beta+1)/(3\beta+1)} g^{-(\beta+3)/(3\beta+1)}, \quad (7)$$

and, in turn, the intrinsic cut-off frequency (in the observer frame) can be estimated as  $\nu_c = (3/4\pi)\delta\gamma_c^2[eB_m/(mc)](\lambda_c/d)^{(\beta-1)/2}$ , which is found to be recast in the simple form

$$\nu_c = 27\pi(\beta' - 1)\delta a^{\beta'-1} b \frac{r-1}{r} \frac{mc^3}{e^2}, \quad (8)$$

independent of  $\beta$ ,  $B_m$ ,  $d$ , etc. For  $\beta' = 5/3$ , the quantities scale as

$$\gamma_c = 3.8 \times 10^8 a^{3/7} \xi_{-5}^{3/7} B_m^{-2/7} d^{1/7} \quad (9)$$

for  $\beta = 2$  (see Montgomery & Liu 1979 as an example) and

$$\nu_c = 4.5 \times 10^{19} a^{2/3} \delta \xi_{-5} \text{ Hz} \quad (10)$$

respectively. Note that equation (10) is independent of  $\beta$ . In the ordinary case in which the diffuse emission level is lower

(cf. the discussion in Honda & Honda 2007), equation (10) (instead of equation 2) provides the observed cut-off frequency of the synchrotron radiation, which is of non-diffuse at least in the scale of  $\sim \lambda_c$ . Note that the absorption in extragalactic background lights is expected to be insignificant, as long as the radiation frequency is in the range below  $\sim 10^{24}$  Hz (e.g. Kneiske et al. 2004).

### 2.3 The smearing effect on the spectrum at $\nu_c$

The large  $\nu_c$  value expected in equation (10) is owed to the efficient acceleration of electrons bound to the local magnetic fields of filaments with size-scale  $\sim \lambda_c$ . In this regime, the time-scale of escape from a small-scale filament competes with the radiative loss time-scale, and therefore we provide additional discussions concerning the spatiotemporal property of diffusion loss, in order to identify the value of  $a$ . The escape is dominated by diffusion across the magnetic field line permeating through the current filaments, so that for the electrons confined within radial size  $\sim \lambda/2$ , the escape time is estimated as  $t_{\text{esc}} \sim (\lambda/2)^2/c\ell_{\perp}$ , where  $\ell_{\perp}$  is the mean free path (mfp) for diffusion perpendicular to the magnetic field line (e.g. Hillas 1984). Recall that the perpendicular diffusion is characterized by the coefficient  $\kappa_{\perp} = \kappa_{\parallel}/(1 + \eta^2)$ , where  $\eta = \ell_{\parallel}/r_g$ ,  $\kappa_{\parallel} = \frac{1}{3}\eta r_g c$  and  $\ell_{\parallel} = r_g/[b(\beta' - 1)][\lambda/(2r_g)]^{\beta'-1}$  (for  $\beta' > 1$ ) denotes the mfp for the diffusion parallel to the field line (e.g. Mücke & Protheroe 2001; Honda & Honda 2005b). Along with this, we invoke the relation  $\ell_{\perp} \simeq \eta^{-2}\ell_{\parallel}$  for  $\eta^2 \gg 1$ , which is the region of interest to us, and then the escape time can be expressed as  $t_{\text{esc}} = (\ell_{\parallel}/c)(\lambda/2r_g)^2$ . As a result, we find that equating  $t_{\text{esc}}$  to  $t_{\text{acc}}$  correctly provides the aforementioned spatial limit equation in the form of  $r_g = a(\lambda/2)$ , where

$$a = \sqrt{(r-1)}/r. \quad (11)$$

One can ascertain that equation (11) is also valid for  $\beta' = 1$  (not shown). In the strong-shock limit we have  $a = 0.87$ , and suggest that setting  $a$  to unity is nearly adequate for the simple treatment of escape loss. In the case in which the mfp related to the diffusion considered is anomalously longer than the estimated range of  $\ell_{\perp}$ , the  $a$  value becomes effectively smaller than that of equation (11); i.e.  $\gamma_c$  and  $\nu_c$  could reduce, even if the inverse Compton (IC) and redshift effects considered later are negligible. The uncertainty in  $a$  is expected to cooperate to smear out the actual spectrum around  $\nu_c$ .

### 2.4 The inverse Comptonization effect

There exists another possible effect that prevents electrons from being energized up to the range given in equation (9). The starlight and dust emission that emanate from host galaxies potentially serve as external targets for the inverse Comptonization of accelerated electrons. For relativistic jets, one may consider these and also the cosmic microwave background, because the radiation energy density is boosted in the comoving frame by a factor of  $\Gamma_j^2$  (Stawarz et al. 2003). Particularly in the weaker magnetic intensity regions of  $\lambda \ll d$ , the comoving radiation energy

density (denoted as  $u_{\text{rad}}$ ) could be comparable to the magnetic energy density, so that the time-scale for Thomson scattering loss could compete with that for synchrotron loss. It is pointed out that similar circumstances can appear even for a synchrotron originator, if the non-local effect is significant for radiative transfer. On the other hand, it is unlikely that inverse Comptonization affects the lepton energization to the  $\gamma_c$  level of equation (9), because the Klein-Nishina effect tends to reduce the scattering cross-section (e.g., Honda & Honda 2007). In any case, the competition between these conceivable radiative channels is complicated, dependent on the detailed parameters inherent to sources.

With this aspect in mind, we here simply clarify the maximum level of IC losses that can affect the electron acceleration up to  $\gamma_c$ . For example, one can identify the maximum equivalent IC field (denoted as  $B_{\text{ic}}$ ) corresponding to the quantity  $\sqrt{8\pi u_{\text{rad}}}$  by conservatively taking the balance of  $t_{\text{acc}}$  with the Thomson time-scale at  $\gamma_c$ . Considering the synchrotron limit at  $\gamma_b$ , it is found that any IC losses can safely be ignored (i.e. equations 9 and 10 are valid) if

$$\frac{B_{\text{ic}}}{B_m} < \left( \frac{\gamma_b}{\gamma_c} \right)^{(\beta-1)(3-\beta')/[(\beta+1)\beta'-2]} \quad (12)$$

The criterion for  $(\beta, \beta') = (2, 5/3)$  reduces to  $B_{\text{ic}}/B_m < (\gamma_b/\gamma_c)^{4/9}$ , which would generally be satisfied. In the following, therefore, we are concerned with the negligible contribution of Compton losses to the maximum energy analysis, aiming at providing a generic theoretical upper limit on the (non-diffuse) synchrotron radiation frequency that has not been manifested so far.

### 3 COMPARISON WITH OBSERVATIONAL DATA

#### 3.1 The ageing effect and degenerative $\nu_c$ redshift

We further expand our discussions on the validity of the scalings of  $\nu_b$  and  $\nu_c$ , in light of the comparison with observational data. In equation (6), we have the  $\nu_b$  scaling apparently proportional to  $B_m^{-3/2}$ . However, there is a potential that the correlation length-scale  $d$  is virtually related to  $B_m$ , yielding an explicit magnetic intensity dependence of  $\nu_b$ . To see this, in Fig. 2, we plot magnetic field strength  $B$  against emission-region size  $D$  for 48 sample objects (102 features) that include blazars, Fanaroff-Riley type I/II radio galaxies (denoted as FRI/II, respectively) and quasi-stellar objects (QSOs). It is found that the power-law fitting suggests a generic scaling of  $D \sim B^{-2.1 \sim (-2)}$ , though the translation to a  $d-B_m$  relation is not trivial. At this juncture, provided the scaling is the same, one may read off  $\nu_b \sim B_m^{0.5 \sim 0.6}$ , when supposing a simple ordering of  $B/B_m \lesssim 1$  and that  $d \sim D^{0.7}$  is retained (cf. Section 4), we preliminarily obtain  $\nu_b \sim B_m^{-0.1 \sim +0.1}$ . In any case, the resulting magnetic intensity dependence of  $\nu_b$  is thought of as being weak in the present context. This property appears to be, if it is correct, markedly different from  $\nu_b \propto B^{-3}$  (Brunetti et al. 2003; Cheung et al. 2005), which was derived considering the synchrotron cooling of ageing electrons in hot spots (Meisenheimer et al. 1997). We point out that observations provide some support for the classical scaling (for hotspots), implying that the present analytic results cannot directly be

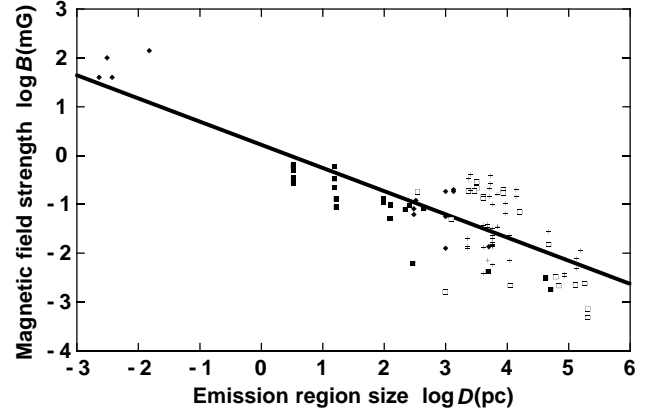


**Figure 2.** Magnetic field strength  $B$ , versus emission-region size  $D$ , for blazars (filled diamonds), FRI (filled squares) and FRII (open squares) radio sources and QSOs (crosses).  $B$  equipartition values in the rest frame, i.e.  $B_{\text{eq},\delta=1} \delta^{-5/7}$ , are from Kataoka & Stawarz (2005) (KS05), except for the marginal data of four compact BL Lacs, which are commonly from the synchrotron self-Compton models provided in the literatures in Table 1. It is noted that for the 'SYN' features classified in KS05,  $B$  is simply set to  $B_{\text{eq},\delta=1}$ . The solid line indicates the best-fitting scaling  $B = 1.7D^{-0.48}$ .

applied to hotspot phenomena, although the applicability of the filament model as such still remains unclear.

In the synchrotron spectrum, the appearance of ageing effects might be pronounced, particularly during the low activity around the working surface, which can be translated as the quenching of turbulent energy injection at the smallest size-scale (i.e. the largest wavenumber,  $k_m$ , in the filamentary turbulent spectrum: Honda et al. 2000). The inertial inverse cascade will lower the upper cut-off  $k_m$ , resulting in a lack of smaller-scale filaments and magnetic energy condensation around the outer scale  $\sim d$ . When entering into the degenerate regime of  $k_m^{-1} > \lambda_c/2\pi$ , equation (10) is violated, and the further cascade leads to the 'redshift' of cut-off frequency moving toward the lower limit compared with the  $\nu_b$  range given in equation (6). This scenario provides a reasonable interpretation of the observational fact that there are still many objects with a cut-off signature around the optical band (e.g. Meisenheimer et al. 1997; Mack et al. 2009), while there is evidence of synchrotron X-ray emission in a number of jets and hotspots (Harris & Krawczynski 2006); i.e. the inspected low-energy cut-offs do not always imply extremely small values of  $\xi$  in equation (10). In the specific regime, a spectral break below the low-energy band could reflect the oldest electron population along the classical scenario, whereupon the scaling of  $\nu_b \propto B^{-3}$  might be realized (Brunetti et al. 2003; Cheung et al. 2005).

#### 3.2 Theoretical upper limit of $\nu_c$

Listed in Table 1 are the relevant data for radio sources, which are used to evaluate the value of  $\nu_c$  in equation (10) and to compare the measured  $\nu_b$  with equation (6). Basically, we have sought X-ray sources that retain the extension of the synchrotron continuum above the confirmed  $\nu_b$ , although

for the data selection the statistical bias might inevitably be involved. The samples selected here include BL Lac objects, FRI radio galaxies, core-dominated quasars (CDQ) and a gamma-ray quasar (GRQ); these are found, in particular, to provide a well-defined parameter set that could also be referred to the correlation length estimate later in equation (13). Taking a conservative approach, FR II sources have been excluded at the moment, since hotspot phenomena in the tips often incur the ageing effects that have been annotated in Section 3.1, and also show some peculiar features in energetic emission (e.g. Pic A; Tingay et al. 2008). On the other hand, there are some cases for which FR II features resemble knots in jet (e.g. Meisenheimer et al. 1997; Marshall et al. 2010), and therefore the applicability of the present model to FR II sources will be investigated in more detail, though it seems to be somewhat beyond the scope of this paper.

The updated X-ray data provide the lower limits on  $\nu_c$  in equation (10), and thereby the lower limits of the unfixed parameter,  $\xi_{\min}$ , for given  $a \sim 1$  (upper limit) and measured  $\delta$  values. Then, by invoking a simple relation  $p \sim (r+2)/(r-1)$  (see Schlickeiser 2002, for details), the lower limits of  $b$  can be estimated such that  $b_{\min} \sim [(p+2)/4]\xi_{\min}$ .

Fig. 3 plots the predicted values of  $\nu_c$  against  $b$  (in the range of  $\geq b_{\min}$ ), except for CDQs (for reasoning, see Section 4). According to equation (11), the value of  $a$  is simply set to  $\sqrt{3/(p+2)}$  hereafter. It is confirmed that the condition of  $b \ll 1$  (introduced in Section 2.2) is satisfied as long as  $\nu_c \leq 10^{23}$  Hz. For a given  $b$ , the  $\nu_c$  values of the compact BL Lacs are likely higher than those of the FRI sources, mainly because of the higher  $\delta$  values for the BL Lacs. For the set  $(p, \delta) = (1.6, 10)$  (Mrk 421, Mrk 501: e.g. Tavecchio et al. 2001; Konopelko et al. 2003; Błażejowski et al. 2005), a specified value of  $b = 1 \times 10^{-3}$  yields  $\nu_c = 4.7 \times 10^{22}$  Hz, in conformity with the extremely high-frequency ranges of synchrotron cut-off expected in TeV gamma-ray emitters (Honda 2008). It is also mentioned that the scaling of a beaming GRQ (PKS 0208-512 with a hundred-kpc scale; Schwartz et al. 2006) appears to be close to that of a kpc-scale BL Lac (3C 371: Pesce et al. 2001, not shown in the figure).

#### 4 CORRELATION LENGTH-SCALE AND ‘PACKAGE’ OF FILAMENTS

A worthwhile manipulation is to combine equation (6) with (10), eliminating the parameter  $\xi$ . We solve this for the correlation length  $d$  to find the scaling

$$d = 5.4 \times 10^{-3} a^{-1} \delta^{-1/2} \nu_{b,14}^{-1} \nu_{c,17}^{3/2} B_m^{-3/2} \text{ pc}, \quad (13)$$

where  $\nu_{b,14} = \nu_b/10^{14}$  Hz and  $\nu_{c,17} = \nu_c/10^{17}$  Hz. By putting the parameter values of Table 1 into the right-hand side of equation (13), one can fix the allowed  $d$  domain for each sources. In the derivation of equation (13), it is supposed that the parameter  $\xi$  in equations (6) and (10) takes a common value (cf. Honda 2008). If the back-reaction effect of accelerated particles on the shock structure (e.g. Blasi 2002; Kang & Jones 2007) comes into play with a positional dependence, the value of  $\xi$  may be different in between the regions of  $\lambda \sim d$  and  $\lambda_c$ , as  $b$  and  $r$  change spatially. Related to this issue, the strong non-linear effect also invalidates the

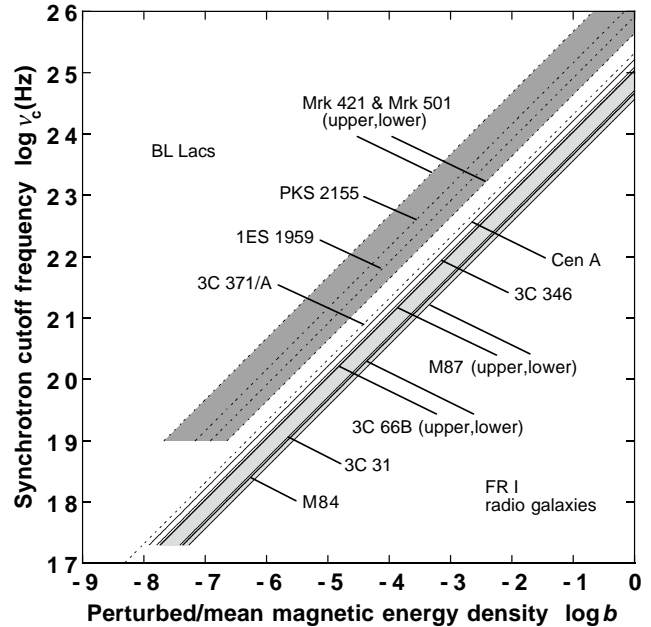


**Figure 3.** The cut-off frequency  $\nu_c$  of synchrotron emission from the extragalactic jets (labelled) as a function of the energy density ratio of the perturbed/local mean magnetic field of filaments,  $b$ . The darkly and lightly shaded areas indicate the expected domains for Mrk 421 and 501 with  $(p, \delta) = (1.6 - 1.8, 10 - 100)$  and M87 with  $(2.3, 1 - 3)$ , respectively.

assumption of  $b \ll 1$  followed by  $\eta \gg 1$ . We mention here that the back-reaction effect may scatter the results shown below, resulting in an effective lower estimate of  $d$  (in equation 13), but quasi-linearity ( $b \ll 1$ ) seems to be almost satisfied even in the smaller filament with  $\lambda_c$ , at which the acceleration efficiency is maximum.

Fig. 4(a) plots the lower limit,  $d_{\min}$ , against the size of emission region  $D$ . Note the relation  $d_{\min} < D$ , which maintains the theoretical consistency. As seen in the figure, the plotted points including bars may be separated roughly into three groups (labelled as BL Lac, FRI and CDQ). Notice that the FRI group apparently absorbs a large-scale BL Lac (3C 371), implying the similarity of turbulent states. Although the uncertainty ascribed to the observations is not small for the moment, it seems natural to suppose that the  $(D, d_{\min})$  points of the BL Lac and FRI share a common power-law scaling. The CDQ group is apparently isolated in a marginal region below the scaling (mainly because of the larger uncertainty of  $\nu_c$ , stemming from the flat spectral features; cf. Table 1), although the  $d_{\min}$  levels are still retained above a skin depth for the plasma density of  $> 10^{-6} \text{ cm}^{-3}$ , satisfying the restriction  $\lambda/d_{\min} \leq 1$  (consistent with the filamentation instability; Honda et al. 2000). With the exception of the marginal data, the power-law fitting yields a scaling of  $d_{\min, \text{pc}} \sim 5 \times 10^{-5} D_{\text{pc}}^{0.7}$ , where the units are pc. This arguably reflects the history of how the filamentary turbulence evolves as the jet propagates, increasing the width. The physical implication can be revealed by translating a quantity  $\lesssim D^2/d_{\min}^2$  as the upper limit of the number of outer-scale filaments,  $(N_{\lambda \sim d})_{\max}$ .

**Table 1.** Sample parameters to evaluate equations (10) and (13).

Host/feature (class)	$D(\text{pc})^a$	$p^b$	$B_m(\text{mG})^c$	$\delta$	$\nu_b(\text{Hz})$	$\nu_c(\text{Hz})$	References <sup>d</sup>
1ES 1959+650 (BL Lac)	$3.8 \times 10^{-3}$	2	400	20	$10^{16} - 10^{17}$	$\geq 10^{19}$	1
Mrk 421 (BL Lac)	$3.1 \times 10^{-3}$	1.75	1000	55	$10^{16}$	$> 10^{19}$	2,3
Mrk 501 (BL Lac)	$2.3 \times 10^{-3}$	1.60	400	50	$10^{16}$	$\geq 10^{20}$	2,4
PKS 2155-304 (BL Lac)	$1.5 \times 10^{-2}$	1.35	1400	28	$(.5 - 1.3) \times 10^{16}$	$> 10^{19}$	5,6,7,8
3C 371/A (BL Lac)	252	2.52	.81	6	$10^{14} - 10^{15}$	$> 10^{17}$	9,10,11
M84/N3.3 (FRI)	8	2.3	1.3	.6 - 1.25	$4 \times 10^{13}$	$> 2 \times 10^{17}$	10,11,12
3C 31 (FRI)	68	2.1	1.1	1.3	$10^{13}$	$\geq 2 \times 10^{17}$	10,11,13
3C 66B/B (FRI)	85	2.2	1.2	1.2 - 2.8	$10^{14}$	$> 2 \times 10^{17}$	11,14,15
M87/A (FRI)	110	2.34	5.1	1 - 3	$(.27 - 7.0) \times 10^{16}$	$> 2 \times 10^{17}$	16,17,18,19,20
Cen A (FRI)	154	2	6.4	4	$10^{12} - 10^{14}$	$\geq 2 \times 10^{17}$	10,11,21,22
3C 346 (FRI)	320	2	7.2	$< 3$	$10^{12} - 10^{13}$	$\geq 2 \times 10^{17}$	11,23
PKS 0208-512/R2 (GRQ)	5240	2.4	.135	7.5	$\leq 10^{14}$	$\geq 10^{17}$	11,24,25
3C 273/D (CDQ)	3000	2.6	220	4.2	$10^{13} - 10^{14}$	$> 10^{15}$	26,27
4C 49.22/B (CDQ)	7800	2.4	.75	14	$10^{13} - 10^{14}$	$> 10^{15}$	10,11,28
4C 19.44/A (CDQ)	10000	2.4	.86	14	$10^{13}$	$> 10^{15}$	10,11,28
PKS 1202-262/R2 (CDQ)	11400	2.4	120	12	$10^{11} - 10^{14}$	$\geq 10^{15}$	11,25
PKS 1030-357/R2 (CDQ)	13600	2.4	223	9.2	$10^{11} - 10^{14}$	$\geq 10^{15}$	11,25
PKS 0637-752 (CDQ)	16700	2.62	2	10	$< 3 \times 10^{12}$	$\geq 5 \times 10^{14}$	11,29,30

<sup>a</sup> Values set simply to  $D = L/50$ , if not well defined.

<sup>b</sup> Values inferred from comparing the measured radio spectral indices with  $\alpha = (p - 1)/2$ .

<sup>c</sup> For an ad hoc manner, set to ten times the field strength suggested in Refs (for the reasoning, cf. Honda 2008).

<sup>d</sup> Ref: 1. Krawczynski et al. 2004, 2. Konopelko et al. 2003, 3. Błażejowski et al. 2005, 4. Tavecchio et al. 2001, 5. Urry et al. 1997, 6. Kataoka et al. 2000, 7. Zhang et al. 2002, 8. Dominici et al. 2004, 9. Pesce et al. 2001, 10. Kataoka & Stawarz 2005, 11. Harris & Krawczynski 2006, 12. Harris et al. 2002, 13. Hardcastle et al. 2002, 14. Tansley et al. 2000, 15. Hardcastle et al. 2001, 16. Owen et al. 1989, 17. Biretta et al. 1991, 18. Perlman et al. 2001, 19. Marshall et al. 2002, 20. Waters & Zepf 2005, 21. Kataoka et al. 2006, 22. Hardcastle et al. 2006, 23. Worrall & Birkinshaw 2005, 24. Whiting et al. 2003, 25. Schwartz et al. 2006, 26. Sambruna et al. 2001, 27. Jester et al. 2002, 28. Sambruna et al. 2004, 29. Schwartz et al. 2000, 30. Chartas et al. 2000.

Fig. 4(b) plots the values of  $(N_{\lambda \sim d})_{\max} (= D^2/d_{\min}^2)$ , for convenience) as a function of the deprojected length of jets  $L$ . Interpolating them yields the scaling  $(N_{\lambda \sim d})_{\max} \sim 10^9 L_{\text{kpc}}^{0.6}$ , indicating the trend that the capacity of outer-scale filaments increases as  $L$  increases (shaded area). In order to see the significance, we recall a promising scenario in which jets having large-scale magnetic fields are necessarily accompanied by huge currents in the bulk plasmas (Appl & Camenzind 1992), the kinetic energy of which is dissipated only a little during the transport from the cores to the lobes (Tashiro & Isobe 2004). As a whole, this is compatible with the superconductivity of plasmas.

For example, let us consider the well-confirmed samples M87 and Cen A, the nuclei of which have the super-massive black holes with mass  $\sim 10^9 M_{\odot}$  (Macchetto et al. 1997) and  $(10^7 - 10^8) M_{\odot}$  (Marconi et al. 2006), respectively. According to the arguments of Appl & Camenzind (1992), their central engines, incorporated with their accretion discs, ought to have the potential to drive a current of the order of magnitude of  $I \sim 10^{19}$  A and  $\sim 10^{18}$  A, respectively. Such a huge current could not be transported by a single uniform column, on account of the current inhibition (Honda 2007). One possible solution is to allow for the presence of many filaments that each carry a current limited by  $i_0 \sim (mc^3/e)\beta_j\Gamma_j$  (Honda 2000). It is noted that the value of  $i_0$  is independent of  $\lambda$  (Honda et al. 2000). The number of current filaments can then be estimated as  $N(\sim I/i_0) \sim 10^{15}$  and  $\sim 10^{14}$ , respectively. Note that these values are just in

the expected ranges of  $(N_{\lambda \sim d})_{\max}$  for M87 and Cen A (cf. Fig. 4b). The outcome suggests that, if the actual capacity of the outer-scale filaments reaches the level  $\sim (N_{\lambda \sim d})_{\max}$ , the filament cluster, which consists of the smaller filaments with size  $\lambda < d$ , would not be closely packed in the jet. This seems to be qualitatively amenable to the observed appearance of the non-uniformly filled features in the jets of M87 (Biretta et al. 1991; Marshall et al. 2002) and Cen A (Kraft et al. 2002; Hardcastle et al. 2007).

As for the BL Lac object Mrk 421, the black hole mass of which is considered to be  $\sim 10^6 M_{\odot}$  (Xie et al. 1998) or more, one anticipates a current of  $I \gtrsim 10^{17}$  A. Regarding the strongly beaming flow with a narrow viewing angle in which  $\delta \sim \Gamma_j$ , we find the order of  $i_0 \sim 10^4 \delta$  A (in the regime, also note the scaling  $\nu_c \sim b(i_0/e)$  in equation 8). For  $\delta \leq 100$ , we accordingly have  $N \gtrsim 10^{11}$ , which is much larger than  $(N_{\lambda \sim d})_{\max} \sim 10^8$  (Fig. 4b). The relation  $N \gg (N_{\lambda \sim d})_{\max}$ , which is in contrast to  $N \sim (N_{\lambda \sim d})_{\max}$  for the aforementioned FRI sources, can also be found in other BL Lacs (Mrk 501, for example). It is thus ensured that the jets accompanying these compact objects have many filaments smaller than  $d$  (and thereby, smaller than  $D$ ), consistent with the assumption given in Honda (2008).

## 5 DISCUSSION AND CONCLUSIONS

Another signature of the 'quantization' of magnetized current filaments can be speculatively found in Fig. 2. By in-

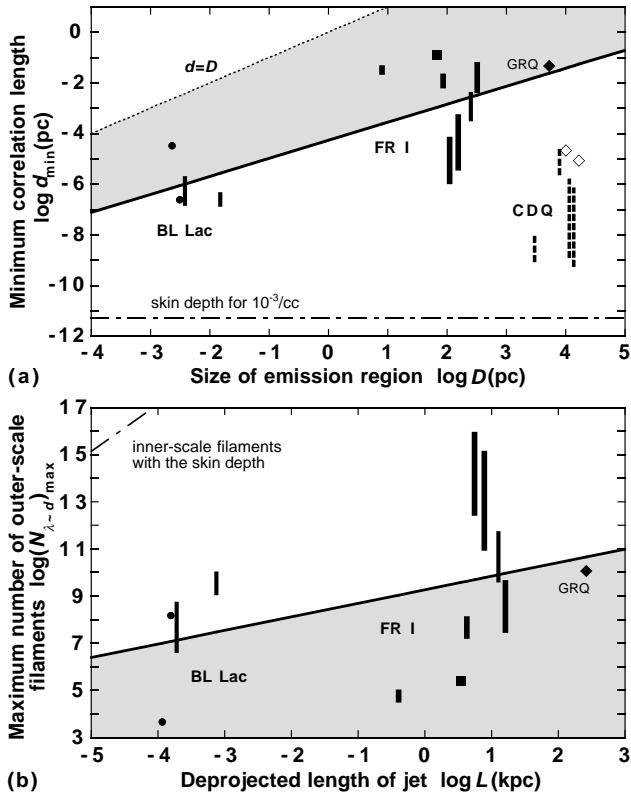


**Figure 4.** (a) The lower limit of the transverse correlation length of filamentary turbulence  $d_{\min}$  versus the emission-region size  $D$ . The shaded area between the spatial limit (dotted line) and a power-law scaling (solid line) indicates the allowed domain for the correlation length. A skin depth is also indicated (e.g. for a plasma density of  $10^{-3} \text{ cm}^{-3}$ ; dot-dashed line). (b) The maximum number of outer-scale filaments  $(N_{\lambda \sim d})_{\max}$  versus the deprojected length of the jet  $L$ . The shaded area (below the scaling; solid line) suggests the capacity of the outer-scale filaments. The dot-dashed line indicates an upper limit:  $D^2$  divided by the square of the skin depth (for  $10^{-3} \text{ cm}^{-3}$ ). BL Lac: circles, bars; FR I: filled square, fat bars; GRQ: filled diamond; CDQ: open diamonds, dotted bars.

voking an approximate scaling  $B \propto D^{-1/2}$ , we find that the column energy density of the magnetic field  $\epsilon_b$ , estimated as  $\sim B^2 D / 8\pi$ , is nearly constant:

$$\epsilon_b (= \text{const.}) \sim 10^{11 \sim 12} \text{ ergs cm}^{-2}. \quad (14)$$

Obviously, this is at odds with the intuitive prediction of  $\epsilon_b \propto D^{-2}$  reflecting three-dimensional (3D) adiabatic expansion, implying that 2D expansion, arguably in the transverse plane, is preferentially inhibited due to the pressure of the large-scale magnetic field that would act radially inward (e.g. Honda 2009). At the same time, it is also suggested that the inhomogeneous magnetic fields in the interior of emission regions robustly sustain such an averaged energy-density level against the self-contraction pressure. Considering this aspect, the degenerate nature reflected in equation (14) might be ascribed to the reasoning that any magnetized filaments can by no means overlap spatially (or occupy the common space) so as to carry a summed current exceeding the critical, quantized value of  $i_0$  [for  $\Gamma_j \gtrsim \mathcal{O}(1)$ ], to

prevent unlimited collapse (Honda 2000; Honda et al. 2000). We note that this exclusive property could not be deduced from the classical hydrodynamic description of current coalescence, according to which an archetypical  $\mathbf{J} \times \mathbf{B}$  pinch leads to self-similar collapse (e.g. Zhdanov & Vlasov 1998). The analogy to the updated notion can be found in the real mechanism for the Fermi pressure in degenerate matter, based on the Pauli exclusion principle (e.g. Chandrasekhar 1967). With this insight, the  $B - D$  property revealed in Fig. 2 can be regarded as a macroscopic appearance of the quantization in relativistic flowing plasmas (Fig. 1), and the beamed emission with  $\nu_c (\lesssim i_0/e$ ; Section 4) as an acute appearance of collective quanta. The origin of the  $\epsilon_b$  value as such (in equation 14) is another issue of note, but the details are beyond the scope of this paper.

In conclusion, in the context of the filamentary jet model, we have analytically provided a new scaling of the cut-off frequency  $\nu_c$  of non-diffuse synchrotron emissions (equation 10). The arguments expanded here are based on the plausible assumption that small-amplitude magnetic fluctuations are superimposed on the local mean fields that permeate through current filaments. It has been demonstrated that the  $\nu_c$  level could be much higher than the previously suggested one (equation 1), consistent with many X-ray measurements. The expected range of the present break frequency (equation 6) appears to be comparable to the previous 'cut-off' (in the nomenclature of earlier literatures). In terms of the validity, we have provided extended discussions of the smearing effect on the synchrotron spectrum at  $\nu_c$ , the inverse Comptonization effect and the ageing effect, which could involve the degenerative redshift of  $\nu_c$ .

By combining the results obtained with key observational data of AGN jets, we have found the property that the minimum correlation length of filamentary turbulence is larger for larger objects. In particular, we address the issue that the correlation data for compact BL Lacs and FR I radio sources are likely aligned in a common scaling, probably reflecting the spatiotemporal evolution of AGNs. This trend is amenable to the AGN unification scheme, in which the FR I sources are envisaged as misaligned BL Lacs. From translating the correlation scaling to the number scaling of filaments, we could infer how the filaments are packaged in the jet interior, and extract the consequence that the current carrying AGN jets must possess many filaments smaller than the entire emission-region size; e.g. for a pc-scale blazar jet the number of filaments is  $\sim 10^{11}$  and more. The findings, including a constant column magnetic energy density, support the conjecture that AGN jets ubiquitously involve filamentary morphology.

## REFERENCES

- Appl S., Camenzind M., 1992, A&A, 256, 354  
 Biermann P. L., Strittmatter P. A., 1987, ApJ, 322, 643  
 Biretta J. A., Stern C. P., Harris D. E., 1991, AJ, 101, 1632  
 Blasi P., 2002, Astroparticle Phys., 16, 429  
 Błażejowski M. et al., 2005, ApJ, 630, 130  
 Brunetti G., Mack K.-H., Prieto M. A., Varano S., 2003, MNRAS, 345, L40  
 Celotti A., Ghisellini G., 2008, MNRAS, 385, 283

- Chandrasekhar S., 1967, *An Introduction to the Study of Stellar Structure*. Dover, New York
- Chartas G. et al., 2000, *ApJ*, 542, 655
- Cheung C. C., Wardle J. F. C., Chen T., 2005, *ApJ*, 628, 104
- Dominici T. P., Abraham Z., Teixeira R., Benevides-Soares P., 2004, *ApJ*, 128, 47
- Gaisser T. K., 1990, *Cosmic Rays and Particle Physics*. Cambridge Univ. Press, New York
- Hardcastle M. J., Birkinshaw M., Worrall D. M., 2001, *MNRAS*, 326, 1499
- Hardcastle M. J., Worrall D. M., Birkinshaw M., Laing R. A., Bridle A. H., 2002, *MNRAS*, 334, 182
- Hardcastle M. J., Kraft R. P., Worrall D. M., 2006, *MNRAS*, 368, L15
- Hardcastle M. J. et al., 2007, *ApJ*, 670, L81
- Harris D. E., Krawczynski H., 2006, *ARA&A*, 44, 463
- Harris D. E., Finoguenov A., Bridle A. H., Hardcastle M. J., Laing R. A., 2002, *ApJ*, 580, 110
- Hillas A. M., 1984, *ARA&A*, 22, 425
- Honda M., 2000, *Phys. Plasmas*, 7, 1606
- Honda M., 2007, *MNRAS*, 376, 871
- Honda M., 2008, *ApJ*, 675, L61
- Honda M., 2009, *ApJ*, 706, 1517
- Honda M., Honda Y. S., 2004, *ApJ*, 617, L37
- Honda M., Honda Y. S., 2005a, *ApJ*, 633, 733
- Honda Y. S., Honda M., 2005b, *MNRAS*, 362, 833
- Honda M., Honda Y. S., 2007, *ApJ*, 654, 885
- Honda M., Meyer-ter-Vehn J., Pukhov A., 2000, *Phys. Plasmas*, 7, 1302
- Jester S., Röser H.-J., Meisenheimer K., Perley R., 2002, *A&A*, 385, L27
- Kang H., Jones T. W., 2007, *Astroparticle Phys.*, 28, 232
- Kataoka J., Stawarz L., 2005, *ApJ*, 622, 797
- Kataoka J., Takahashi T., Makino F., Inoue S., Madejski G. M., Tashiro M., Urry C. M., Kubo H., 2000, *ApJ*, 528, 243
- Kataoka J., Stawarz L., Aharonian F., Takahara F., Ostrowski M., Edwards P. G., 2006, *ApJ*, 641, 158
- Keel W. C., 1988, *ApJ*, 329, 532
- Kneiske T. M., Bretz T., Mannheim K., Hartmann D. H., 2004, *A&A*, 413, 807
- Konopelko A., Mastichiadis A., Kirk J., de Jager O. C., Stecker F. W., 2003, *ApJ*, 597, 851
- Kraft R. P., Forman W. R., Jones C., Murray S. S., Hardcastle M. J., Worrall D. M., 2002, *ApJ*, 569, 54
- Krawczynski H. et al., 2004, *ApJ*, 610, 151
- Lobanov A. P., Zensus J. A., 2001, *Sci*, 294, 128
- Longair M. S., 1994, *High Energy Astrophysics, Vol. 2: Stars, the Galaxy and the Interstellar Medium*. Cambridge Univ. Press, Cambridge
- Macchetto F., Marconi A., Axon D. J., Capetti A., Sparks W., Crane P., 1997, *ApJ*, 489, 579
- Mack K.-H., Prieto M. A., Brunetti G., Orienti M., 2009, *MNRAS*, 392, 705
- Marconi A., Pastorini G., Pacini F., Axon D. J., Capetti A., Macchetto D., Koekemoer A. M., Schreier E. J., 2006, *A&A*, 448, 921
- Marshall H. L., Miller B. P., Davis D. S., Perlmutter E. S., Wise M., Canizares C. R., Harris D. E., 2002, *ApJ*, 564, 683
- Marshall H. L. et al., 2010, *ApJ*, 714, L213
- Meisenheimer K., Röser H.-J., Schlötelburg M., 1996, *A&A*, 307, 61
- Meisenheimer K., Yates M. G., Röser H.-J., 1997, *A&A*, 325, 57
- Montgomery D., Liu C. S., 1979, *Phys. Fluids*, 22, 866
- Mücke A., Protheroe R. J., 2001, *Astroparticle Phys.*, 15, 121
- Ostrowski M., 1988, *MNRAS*, 233, 257
- Owen F. N., Hardee P. E., Cornwell T. J., 1989, *ApJ*, 340, 698
- Pérez-Fournon I., Colina L., González-Serrano J. I., Biermann P. L., 1988, *ApJ*, 329, L81
- Perlman E. S., Biretta J. A., Sparks W. B., Macchetto F. D., Leahy J. P., 2001, *ApJ*, 551, 206
- Pesce J. E., Sambruna R. M., Tavecchio F., Maraschi L., Cheung C. C., Urry C. M., Scarpa R., 2001, *ApJ*, 556, L79
- Sambruna R. M., Urry C. M., Tavecchio F., Maraschi L., Scarpa R., Chartas G., Muxlow T., 2001, *ApJ*, 549, L161
- Sambruna R. M., Gambill J. K., Maraschi L. M., Tavecchio F., Cerutti R., Cheung C. C., Urry C. M., Chartas G. C., 2004, *ApJ*, 608, 698
- Schlickeiser R., 2002, *Cosmic Ray Astrophysics*. Springer, Berlin
- Schwartz D. A. et al., 2000, *ApJ*, 540, 69
- Schwartz D. A. et al., 2006, *ApJ*, 640, 592
- Stawarz L., Sikora M., Ostrowski M., 2003, *ApJ*, 597, 186
- Tansley D., Birkinshaw M., Hardcastle M. J., Worrall D. M., 2000, *MNRAS*, 317, 623
- Tashiro M., Isobe N., 2004, *Astron. Herald*, 97, 400
- Tavecchio F. et al., 2001, *ApJ*, 554, 725
- Tingay S. J., Lenc E., Brunetti G., Bondi M., 2008, *ApJ*, 136, 2473
- Urry C. M., Padovani P., 1995, *PASP*, 107, 803
- Urry C. M. et al., 1997, *ApJ*, 486, 799
- Waters C. Z., Zepf S. E., 2005, *ApJ*, 624, 656
- Whiting M. T., Majewski P., Webster R. L., 2003, *PASA*, 20, 196
- Worrall D. M., Birkinshaw M., 2005, *MNRAS*, 360, 926
- Xie G. Z., Bai J. M., Zhang X., Fan J. H., 1998, *A&A*, 334, L29
- Zhang Y. H. et al., 2002, *ApJ*, 572, 762
- Zhdanov S. K., Vlasov V. P., 1998, *Plasma Phys. Rep.*, 24, 497

This paper has been typeset from a  $\text{\TeX}$ / $\text{\LaTeX}$  file prepared by the author.